2023

Granular Jamming: Stiffness vs Pressure and Organ Palpation Devices

Christopher H. Quach
University of Central Florida

GRANULAR JAMMING: STIFFNESS VS PRESSURE AND ORGAN PALPATION DEVICES

by

CHRISTOPHER HAN QUACH

A thesis submitted in partial fulfillment of the requirements
for the Honors in the Major program in Mechanical Engineering
in the College of Engineering and Computer Science
at the University of Central Florida
Orlando, Florida

Spring Term, 2023

Thesis Chair: Yuanli Bai, Ph.D

ABSTRACT

The intent of this thesis it to find a correlation between the stiffness of granular jammed particles and the pressure of the vacuum initiating the jamming force. Currently, granular jamming is being used to create palpation simulators for physicians to practice feeling the variety of stiffnesses of organs when healthy or ill. Because granular jamming allows for variable stiffness of any shape, it is an apt phenomenon to simulate the change of rigidity organs like the liver undergoes when diseased. For physicians to correctly identify how stiff the organ must be when using these palpation simulators, there needs to be a way to know how much pressure must be applied to correctly simulate the stiffness of the organ for each specific scenario. This thesis will discuss how pressure affects stiffness by using a three-point bending test. To perform this test, a tubular balloon filled with coffee granules was used to represent the beam. An impact force as well as a hanging force was used to displace the beam. The displacement of the beam is adequate to find the Young's Modulus or stiffness of the beam of granules at different negative pressures provided by the vacuum. It was found that there is a correlation between stiffness and pressure of a granular jammed system. This will allow for future physicians to accurately and consistently use model organs to practice palpation techniques.

TABLE OF CONTENTS

LIST OF FIGURES

LIST OF TABLES

INTRODUCTION

Background

In the early 2000s researchers discovered that the jamming of granular materials could serve as a reversible phase transition between a fluid like state to a solid like state and vice versa. Early forms of granular jamming were tested by moving a large object like a sphere or cylinder through a closed container of granular materials or by using a torsional oscillator emersed in a granular medium [1], [2]. For the next several years much knowledge was gained in terms of the ideal shape and conditions the grains should be in for optimal jamming behavior. However, it was not until around 2015 when granular jamming was beginning to be used in soft robotics. The basics of granular jamming in soft robotics include a vacuum pump connected to a rubber membrane filled with granules. When the vacuum pump is activated, the air will exit out of the membrane and the coffee granules will become tightly connected to each other, thus capable of holding items in place or keeping a certain shape.

Soft Robotics and Medical Devices

Grippers

Granular Jamming in soft robotics has tremendous upside because of its innate ability to achieve variable stiffness in a rapid and safe manner. However, in some robotic applications there is a need for a large supporting force with various changes in direction. The article by Park et al. showed a jamming structure that combined the granular jamming idea with a line of chain jamming chambers to allow for an increase in overall average stiffness and various changes in

direction throughout the chain structure. This multilink hybrid jamming structure was tested and proved to assist in upper body limbs and robotic arms [56]. This idea was also popularized by another group because they found that using this chain structure, we can achieve a long range of stiffness instantaneously, just like human limbs. Because the chain structure splits up the granules that are being jammed, it is not possible to create even longer arms that still can be jammed at the same stiffness [88]. Researchers have combined this idea of using jamming to create arms with soft robotic grippers. By using the jamming idea, it is possible to pick up objects by jamming granules around it, move the object elsewhere with a robotic arm, and place the object back down by decompressing the granules. A team was able to create such a device and compare it with a human's ability to perform daily tasks. They also compared the device with the speed of humans doing the same task [43]. Another group of researchers saw immense potential in granular jamming grippers. They saw how granular jamming takes form of whatever object it is encasing and believes that it can perform highly in picking up odd-shaped objects. They use a "one shot" technique where the gripper encases the object when unjammed and picks up the object when jammed. They also focused on improving the production of the device so that the entire gripper, including the membrane and grains were created by 3D printing [61].

Minimally Invasive Surgery Devices

Recently, minimally invasive surgery (MIS) has become popular among surgeons. However, this type of surgery requires a lot of skill and has many technical limitations [82]. This is because MIS uses tools that limit dexterity. Thus, some people have used soft robotics to solve this problem because of its safe interactions with the human body. More specifically, granular

jamming has become the soft robotic solution to this problem. This way they can use granular jamming to stiffen the mechanism when they need to while also using soft material to ensure safety [67], [78]. This concept has become increasingly successful in laparoscopic partial nephrectomy for renal tumors. Previously, the laparoscopic approach for this procedure required tools with high degrees of freedom and low adjustability. However, with these granular jamming MIS devices, the laparoscopic tools can now be reconfigured and jammed to the correct position for long periods of time [68].

Other Medical Devices

An idea has been proposed to improve 3D printing and its stability when printing with liquid. This fluid instability limits the ability for 3D printed objects to hold their shape. Using granular jammed microgels as a medium for printing, it is possible to improve stability even before the printed liquid has solidified [53]. In working with hydrogels, research finds that they seem to mimic biological tissue but lack brittle properties and have poor gelation. However, by jamming the microgels they exhibit shear-thinning and are capable of bridging muscle defects [62], [81].

An interesting interpretation of the benefits of granular jamming lies in the ability to create shapes unique to everyone. This is particularly advantageous in medical devices where the patient must wear a device for long periods of time. For example, orthotic insoles have predetermined unchangeable shapes and properties. With granular jamming, there are now insoles being created so that clinicians can change the stiffness of the orthotic as well as the size

and shape based on the patient [75]. Another concept comes from transnasal skull base surgery where the patient's head must be fixated to maximize accuracy and minimize error. Using granular jamming, a fiducial marker cap has been created for the patient to wear and then granular jam the cap to the head. The fiducial markers on the cap will allow for the surgeon to mark where the patient's head is supposed to be. It can be used and fit everyone perfectly because of granular jamming's ability to take the shape of anything it encases [72].

Controllable Organs

In the medical field, whether it be those in training or experts, tactile hands-on training is important. However, the equipment currently being used is expensive and lacks variability. To combat this, granular jammed controllable organs are being created to simulate different scenarios where medical palpation is necessary and requires haptic training. One party has constructed a granular jamming surface to mimic the abdominal region. They simply tested whether people could tell the difference between different shapes in the "haptic surface" created by granular jamming. They were able to form shapes that could be present in human bodies like hard and soft lumps as well as unnatural shapes like rings. This team has also implemented "ferro granular" jamming by combining magnetic paint with the granules to allow for more control and precision of the grains [6]. More specifically, there has been research done to create a palpation device capable of imitating the stiffness of tumors as well as size and shape. It has been noted by physicians that there is a need for physical contact with the patient to diagnose tumors. To train for this, a granular jamming palpation device has been created to simulate this process. The device includes a nodule that can vary stiffness while maintaining the same shape to mimic

different types of tumors [46]. Like this idea, another research team noticed that there is no entire controllable organ with tumor simulation. This team created a soft robotic controllable liver that can simulate different diseases and symptoms for training all modeled by granular jamming. With granular jamming they were able to simulate inflammation, tumor size, liver stiffness, and liver size. They used rubber balloons and coffee grains to mimic the "craggy" surface of liver tumors. In addition, a specific sample of silicone and softener was created for the liver to match the material stiffness to human liver tissue. This intriguing design was sent to the UK to test at hospitals [86]. Lastly, there has been training done by physicians to regulate palpation forces during a patient's "guarding phase". This phase is when the patient is experiencing discomfort and surface muscles react by contracting. The challenge for physicians is to elicit just enough surface tension without the patient initiating their guarding phase. A group of researchers decided to create a granular jamming palpation simulator with a haptic mouse to help with training. With the haptic mouse, they were able to give feedback on a screen about whether the virtual "patient" was feeling pain. They also combined granular jamming with multiple different layers of glass beads, polystyrene beads, latex layers, and mylar layers to mimic skin and fat layers in the body [90].

Current Status of Granular Jamming

Today, granular jamming is still a relatively new technique and discovery. Thus, the research being done is still varied and minimal. The most popular use of granular jamming is still in soft robotics. Many people have taken a liking to the reversibility between solid and fluid properties

that jammed grains can demonstrate. This has resulted in the creation of granular jammed grippers that can lift oddly shaped items of varying weights that previous robots have had trouble with [61].

Another group of researchers have used this idea and applied it to the medical field. A popular application comes from minimally invasive surgeries (MIS) where the need for a reversible but stable way to hold biological and surgical materials together without hurting the patient has been resolved by granular jamming.

There has also been a large portion of research that has been dedicated to understanding the physics and dynamics behind granular jamming. Before its conception, granular jamming had never been questioned in terms of how and why these grains jam this way and how we can predict the behavior and structure of these jammed grains. Naturally, a way to explain the physics behind jamming was to compare it with different phenomena in science like protein folding and more [71]. The information that was found on granular jamming also created the need to improve and innovate on the topic. Current research is being done on improved methods to granular jamming that expand on the idea. For example, fiber jamming, and twisted rubber jamming have been proposed as an improvement to granular jamming [87], [89].

Statement of Problem

The effect granular jamming has had on soft robotics has been the greatest and most tangible. In particular, the medical field has had improvements in minimally invasive surgery, robotic arm devices, and palpation simulators. For minimally invasive surgery, there is no longer a need for multiple assistants to hold instruments in place because of the increase in stability that granular jamming devices provide. In hospitals, granular jammed arms have provided upper body limb assistance and were even capable of performing human tasks with a gripper attached to the end of the arm. However, palpation simulators need improvements. Palpation simulators can teach current and future physicians what certain tactile changes around the body would feel like because of the variability in stiffness that granular jamming can provide. These palpation simulators can affect the future of physicians and haptic training. Yet, these palpation simulators have yet to be used by doctors because they do not know how to properly measure the stiffness of each organ or tumor when using the palpation simulators. If there was a way to know how to jam the simulator to match the desired stiffness consistently, then the simulators would have a concrete method for training. In addition, we also need to know if the granular jamming palpation simulators can reach the stiffnesses of organs when healthy and diseased.

Scope of the Study

While investigating the correlation between pressure and stiffness of granular jammed systems we included an impact test. Whilst the common practice of palpation testing in the medical field involves rubbing motion rather than a tapping motion which the impact test more closely resembles. However, this test was done solely to test the stiffness through a three-point bending test. Also, as a result, the granular jammed system shape used was a beam rather than organ-shaped because of the requirements for a three-point bending test. In addition, the scope of the study is limited to 10kPa maximum because of the instruments used. Finally, for this experiment granular jamming is defined to use irregular particles for the granular media. Further research may be done to test the effects of using every type of granular media.

IMPACT THREE-POINT BENDING TEST

Introduction

Finding the stiffness of granular jammed systems can be complex because of the different shapes and sizes these systems are made to be. Thus, a uniform shape must be used to have consistent data. If the shape of the system is a beam, it is possible to perform a three-point bending test to find the stiffness of the granular jammed beam. In a three-point bending test, a beam of any material is placed on two pins a certain distance away from each other. A force is then applied to the center of the beam causing the beam to bend. Once the force is finished, it is possible to measure the displacement of the beam from its original position before the force was applied. This displacement can then be applied to the flexural stiffness equation. Flexural Stiffness measures the maximum amount of stress the material experiences. From the flexural stiffness we can finally find the Young's Modulus or also known as the Elastic Modulus which shows us the stiffness of the material. Performing this test for a granular jammed beam at different pressures will give us the stiffness at each different pressure. In this "Impact Three-Point Bending Test", a weight was dropped from a certain height and its impact with the beam was used as the force. We then measured the displacement caused by the falling weight and put it into the flexural stiffness equation and later manipulated this equation to find the Young's Modulus. The flexural stiffness equation is as follows [91]:

$$E_b I = \frac{F_b {L_s}^3}{a\delta} \qquad (1)$$

Where $E_b I$ is the flexural stiffness in Nmm^2, F_b is the bending force in N, L_s is the length between supports in mm^2, a is a constant equal to 48 for three-point bending, and δ is the displacement in mm.

Manipulating this we can find the Young's Modulus as shown below:

$$E_b = \frac{F_b {L_s}^3}{a\delta I} \qquad (2)$$

Where I is the second moment of area in mm^4, and E_b is the Young's Modulus found from the bending in $\frac{N}{mm^2}$, also known as MPa.

To find the second moment of area I, we use the following equation:

$$I = \frac{\pi r^4}{4} \qquad (3)$$

Where r is the radius of the weight face in mm.

Methods and Materials

With the equations set, performing the experiment requires the granular jamming mechanism. To create the jamming mechanism an 18-centimeter-long uninflated balloon was used to hold the coffee granules. The balloon holds 11.5mL of coffee granules but only was filled to 10mL. The type of coffee was Nescafe Instant Coffee because the granule size and shape were conducive for jamming. The coffee filled balloon was then attached and sealed to a tube connected to a 500mL syringe acting as the vacuum. When the syringe is pulled, it takes the air out of the balloon and jams the coffee granules together. An air filter was placed in between the balloon and tube so

that the coffee grains stayed inside. Finally, a third tube was attached to the mechanism by a three-way stopcock to connect an electronic TEKCLOPLUS Air Pressure Manometer. This is needed to know the pressure inside the balloon after the air has been taken out. We used this mechanism to jam the coffee granules at a certain pressure shown by the electronic manometer. The jamming mechanism is shown below:

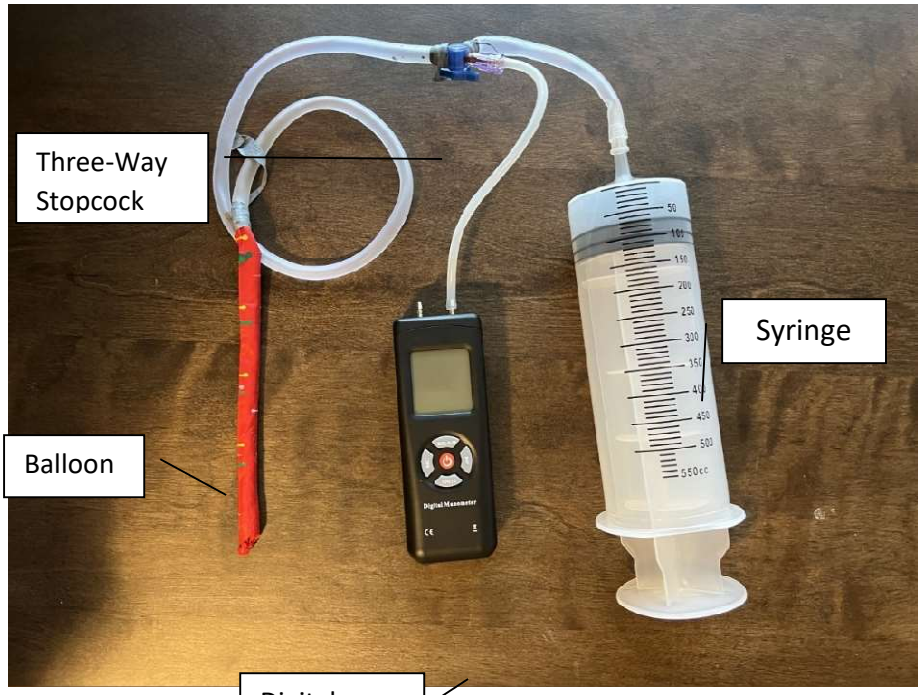

Figure 1: The jamming mechanism [illegible] gital manometer, syringe, tube balloon, and stopcock.

Next, to create the three-point bending test we placed two 4.5cm Styrofoam boxes 10cm away from each other. On the edge of each Styrofoam box, a wooden cylinder was superglued down to act as the supports of the bending. The coffee filled balloon was centered and placed onto the supports. Another support was placed 10cm above the wooden cylinders so that the weight can be dropped from 10cm consistently. The weight was a metal cylinder with a mass of 103.87g, a radius of 12.59mm and a length of 5cm. A string was attached to the weight so that a drop of

10cm would hit the balloon each time. About 2000g of weights were also placed onto the boxes to prevent them from moving at all during testing. Lastly, a laptop with Microsoft Excel was present to record the data of each test. A diagram of the assembled mechanism and weight is shown below:

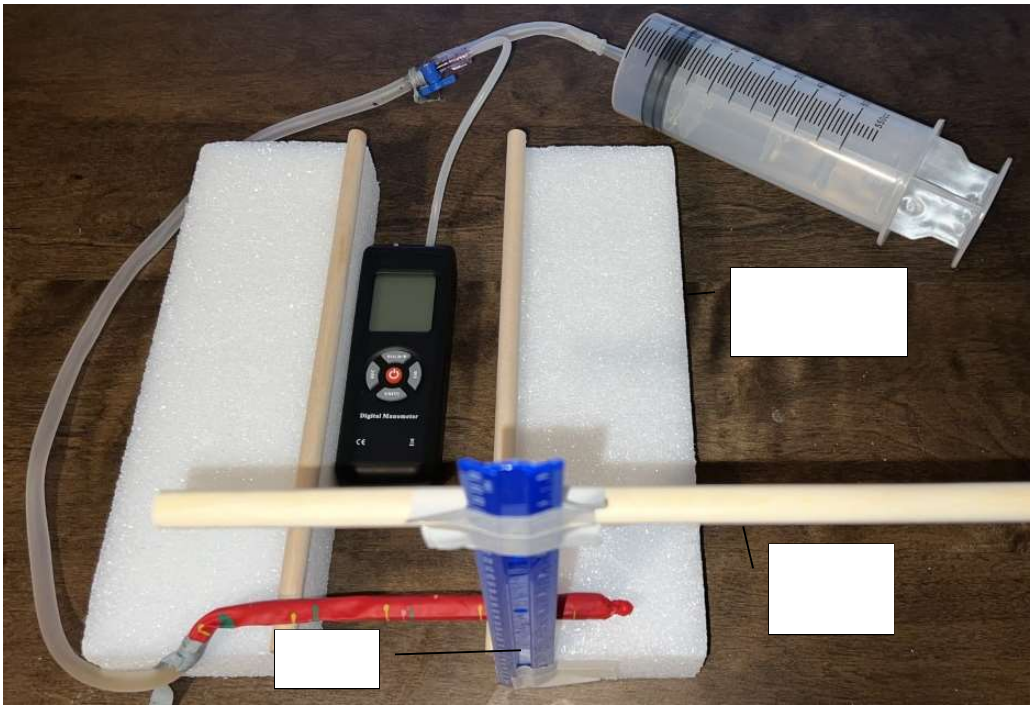

Figure 2: The entire assembled mechanism including the jamming mechanism with the supports and measuring ruler added.

Figure 3: The impact weight measuring as 10cm long including the string, 103.87g, and radius of 12.59mm.

To perform the test, the weight was dropped from the support 10cm high and made an impact with the balloon. The balloon was jammed by the syringe at different pressures. A ruler was attached to the box and a camera recorded each drop. This was to record the initial height of the balloon and final height of the balloon after contact. Subtracting these two values gives us the displacement. The test was done from 0kPa to 10kPa increasing by 0.5kPa each test. The process is shown in the diagrams shown below:


METRIC


METRIC

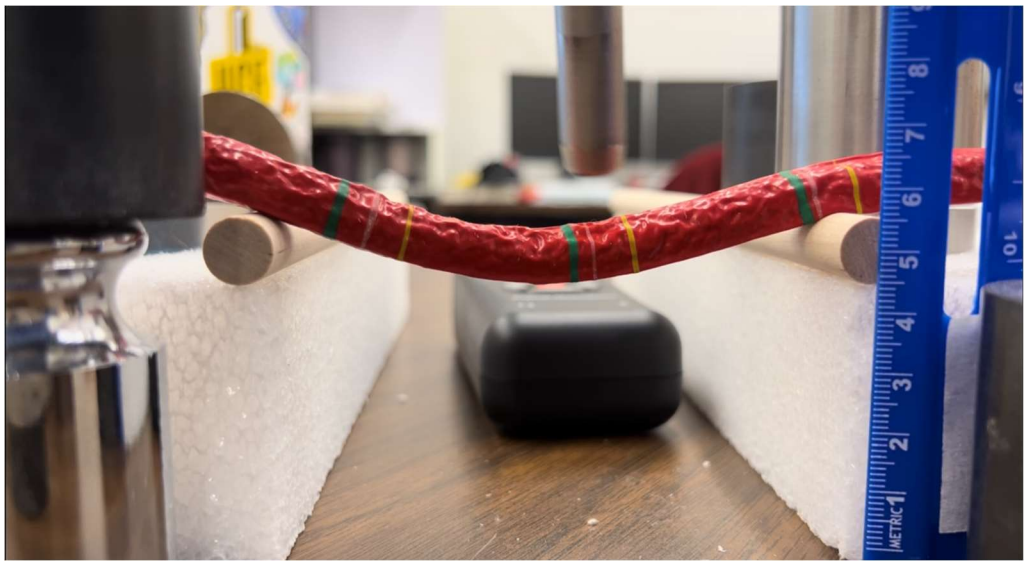

Figure 4: This sample is taken from the 9.5kPa test. This shows the process from unjammed, to jammed, to after impact. This is also how the displacement was measured.

Results

Table 1

Impact Three-Point Bending Test

Pressure (kPa)	Displacement (mm)	Young's Modulus (MPa)	Flexural Stiffness (Nmm^2)
0	48	0.022434934	442.7083333
0.5	45	0.023930597	472.2222222
1	43	0.025043648	494.1860465
1.5	40	0.026921921	531.25
2	37	0.02910478	574.3243243
2.5	36	0.029913246	590.2777778
3	35	0.03076791	607.1428571
3.5	33	0.032632632	643.9393939
4	32	0.033652401	664.0625

4.5	30	0.035895895	708.3333333
5	29	0.037133684	732.7586207
5.5	25	0.043075074	850
6	24	0.044869869	885.4166667
6.5	23	0.046820732	923.9130435
7	20	0.053843842	1062.5
7.5	17	0.063345697	1250
8	15	0.07179179	1416.666667
8.5	13	0.08283668	1634.615385
9	11	0.097897895	1931.818182
9.5	10	0.107687684	2125
10	7	0.153839549	3035.714286

The Young's Modulus and Flexural Stiffness were calcuted using Equations 2 and 1 respectively.

The figures below shows the pressure vs displacement and the pressure vs Young's Modulus

from Table 1:

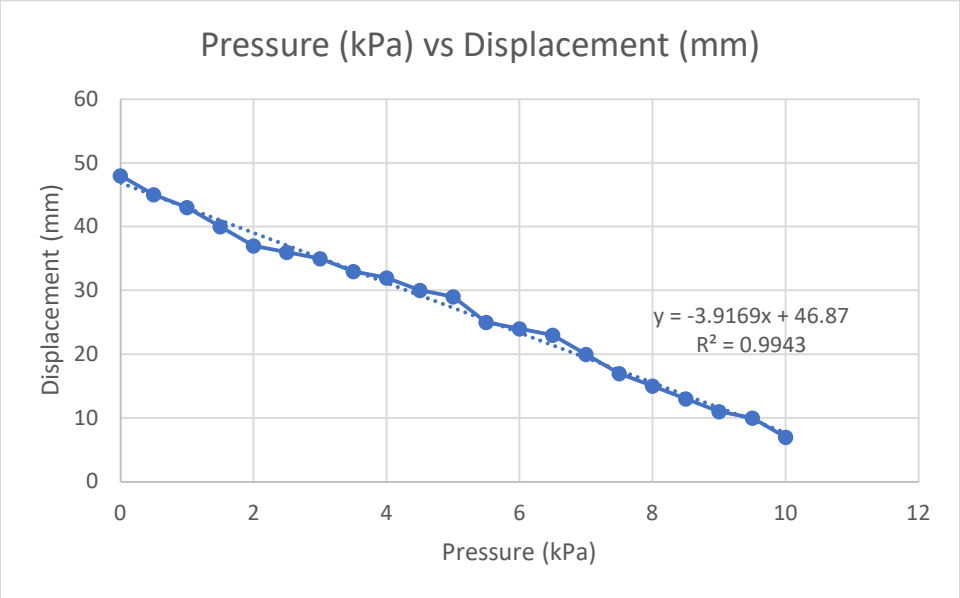

Figure 5: This is the pressure vs displacement of the impact three-point bending test. The line of best fit, line of best fit equation, and the r-squared value were added through Microsoft Excel.

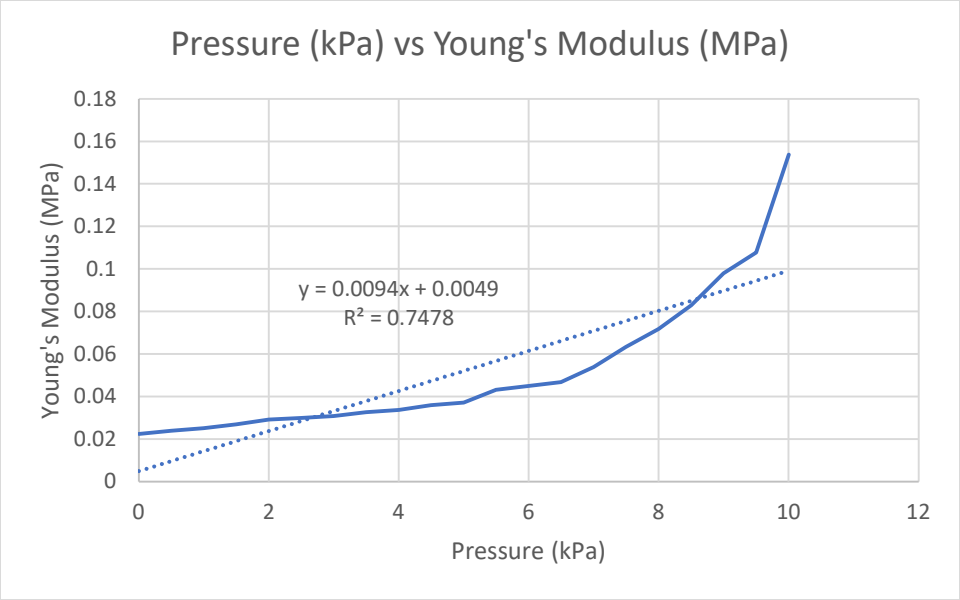

Figure 6: This is the pressure vs Young's Modulus of the impact three-point bending test. The line of best fit, line of best fit equation, and the r-squared value were added through Microsoft Excel.

Discussion

From Figure 5 we see that the pressure and displacement have a clear correlation. As pressure increases, dispalcement decreases at a almost constant linear rate. This is shown to us by the r-squared value of 0.9943 showing an almost perfect correlation. This is expected because it is natural for the balloon to have less displacement after impact with an increase in jamming pressure.

In terms of the Young's Modulus, it seems to have an exponential relationship at first glance. However, it was found that this data contains one outlier at the 10kPa data point as shown below:

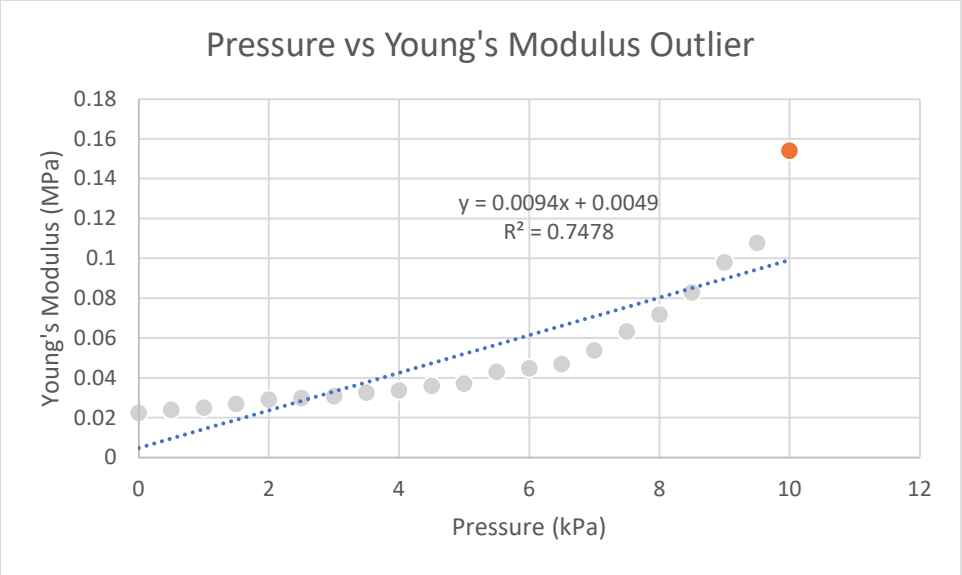

Figure 7: Pressure vs Young's Modulus Data from Figure 6 but highlighting the outlier at 10Kpa.

It is resonable to see how the data changes once this outlier is removed:

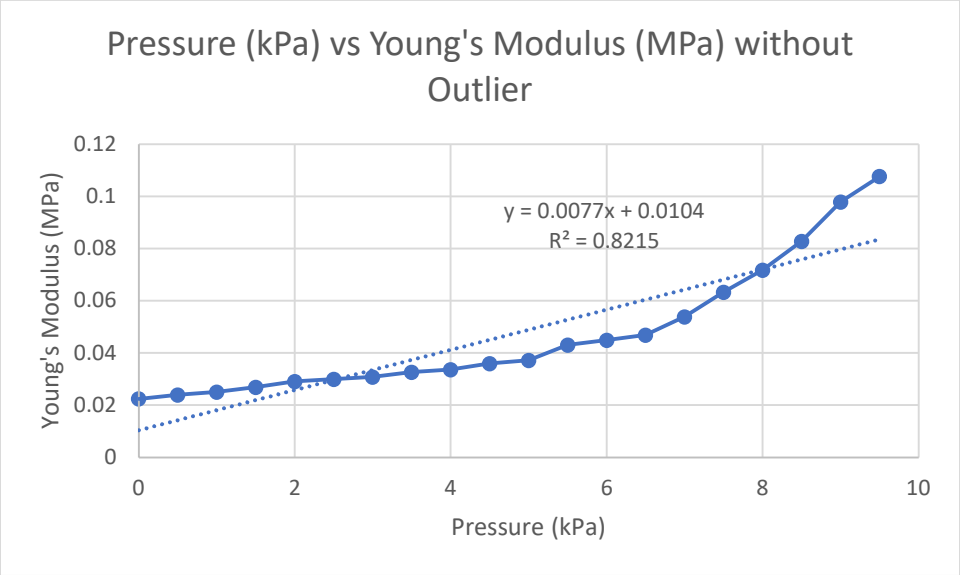

Figure 8: Shows how the Pressure vs Young's Modulus data will change without the outlier.

Note that the r-squared value has increase by 7.37%. Before the outlier was removed there was already a decent linear correlation but after the outlier was removed there is now a good linear correlation.

Next, we will see if the pressure vs Young's Modulus has an exponential correlation. If the exponential correlation is greater than the linear correlation, then we may assume the data is exponential. We do this by taking the natural logarithm of the Young's Modulus and graphing it against the pressure values. This is shown below:

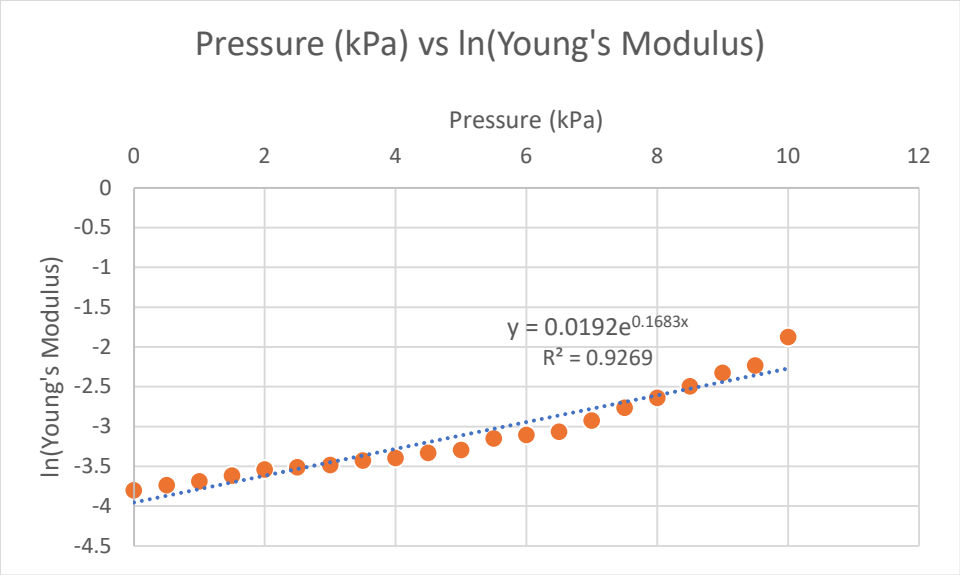

Figure 9: Pressure vs ln(Young's Modulus) with the line of best fit, line of best fit equation, and r-squared value included.

From the Pressure vs ln(Young's Modulus) data we can see that there is a strong linear correaltion from the r-sqaured value of 0.9269. This suggests that there is indeed a exponential

correlation between the pressure data because it has a greater r-squared value than the linear correlation.

HANGING THREE-POINT BENDING TEST

Introduction

In the previous Impact Three-Point Bending Test, it was found that some of the displacement was coming from the force of the impact of the weight rather than just the weight. In other words, the velocity of the falling object was causing most of the displacement. In order to erase this effect, we tried a Hanging Three-Point Bending Test to only account for the weight of the object and to minimize the elastic properties of the materials.

Methods and Materials

In order to conduct the Hanging Three-Point Bending Test, we use the same assembly as Figure 2, however it is now placed over a table edge as shown below:

Figure 10: The entire jamming assembly now placed over a table edge. Note that more weight were added on top of the Styrofoam supports for added stablility.

The assembly was placed over a table edge to allow for the weight to hang from the beam. To perform this experiment, we jam the balloon to a specific pressure and then hang the weight at the center of the beam and allow for the force to only consider the mass of the weight and gravity. We repeat this for every pressure value from 0kPa to 10kPa in 0.5kPa increments (as done in the Impact Test). However, in this case we use a different weight. This new weight has a mass of 12.08g and a radius of 4.81mm as shown below:

Figure 11: The Hanging Weight is shown. Note that we do not need the length of the weight for this experiment because we hang the weight from the side of a table.

After we perform the experiment, we will still use Equations 1, 2 and 3 to find the Young's Modulus and Flexural Stiffness of the jammed balloon. The distance between the supports remains at 10cm and the process is still recorded from the front view to find the displacement afterwards. The process is shown in steps below:

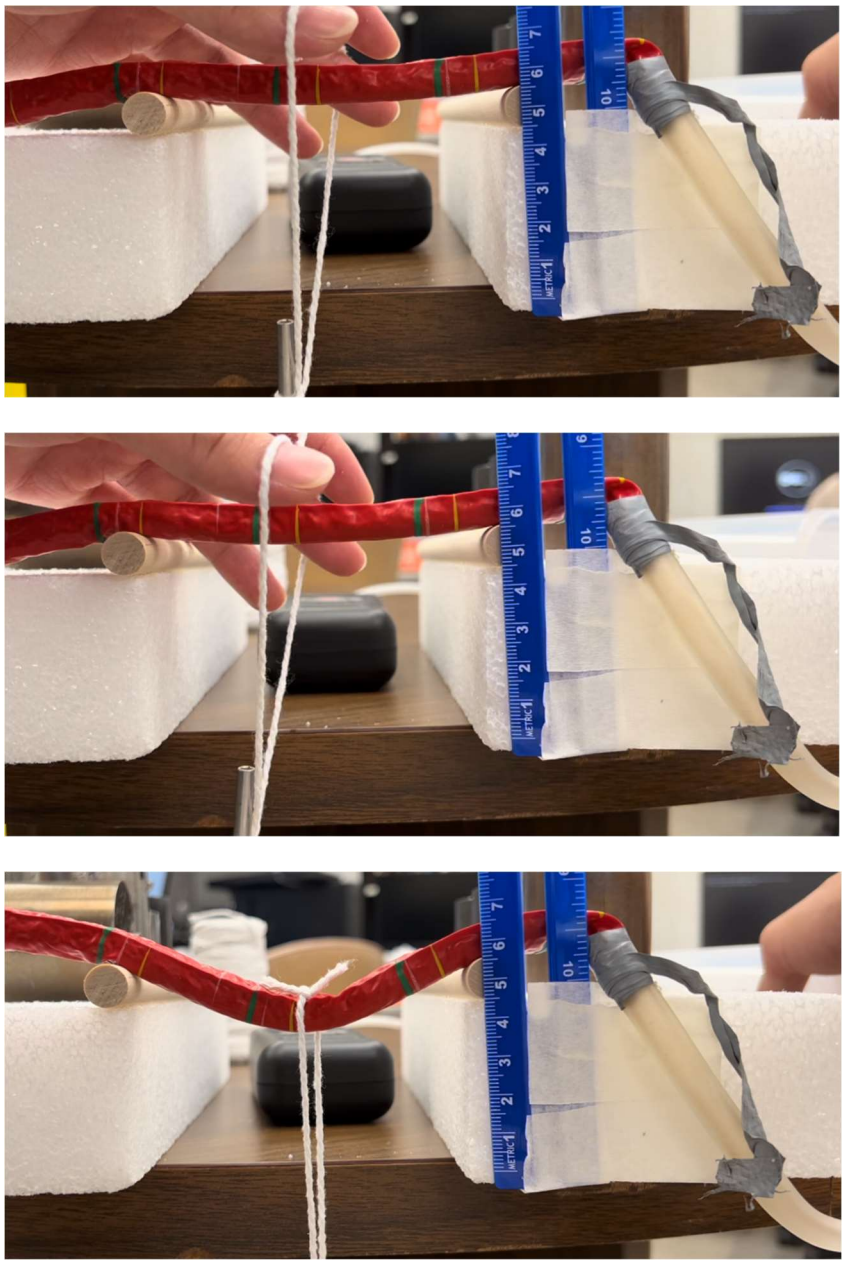

Figure 12: Shows three steps of the Hanging Test: Unjammed, Jammed, and Hanging. The displacement was taken by finding the difference in height when unjammed and the height when hanging.

Results

Table 2

Hanging Three-Point Bending Test

Pressure (kPa)	Displacement (mm)	Young's Modulus (MPa)	Flexural Stiffness (Nmm^2)
0	25	0.23488975	98.75
0.5	19	0.309065461	129.9342105
1	18	0.326235765	137.1527778
1.5	17	0.345426104	145.2205882
2	16	0.367015235	154.296875
2.5	14	0.419445983	176.3392857
3	13	0.451711059	189.9038462
3.5	13	0.451711059	189.9038462
4	12	0.489353647	205.7291667
4.5	11	0.533840342	224.4318182
5	11	0.533840342	224.4318182
5.5	10	0.587224376	246.875
6	8	0.73403047	308.59375
6.5	8	0.73403047	308.59375
7	8	0.73403047	308.59375
7.5	8	0.73403047	308.59375
8	7	0.838891966	352.6785714
8.5	7	0.838891966	352.6785714
9	7	0.838891966	352.6785714
9.5	6	0.978707294	411.4583333
10	6	0.978707294	411.4583333

The Young's Modulus and Flexural Stiffness were calcuted using Equations 2 and 1 respectively.

The figure below shows the pressure vs displacement and pressure vs Young's Modulus of Table 2:

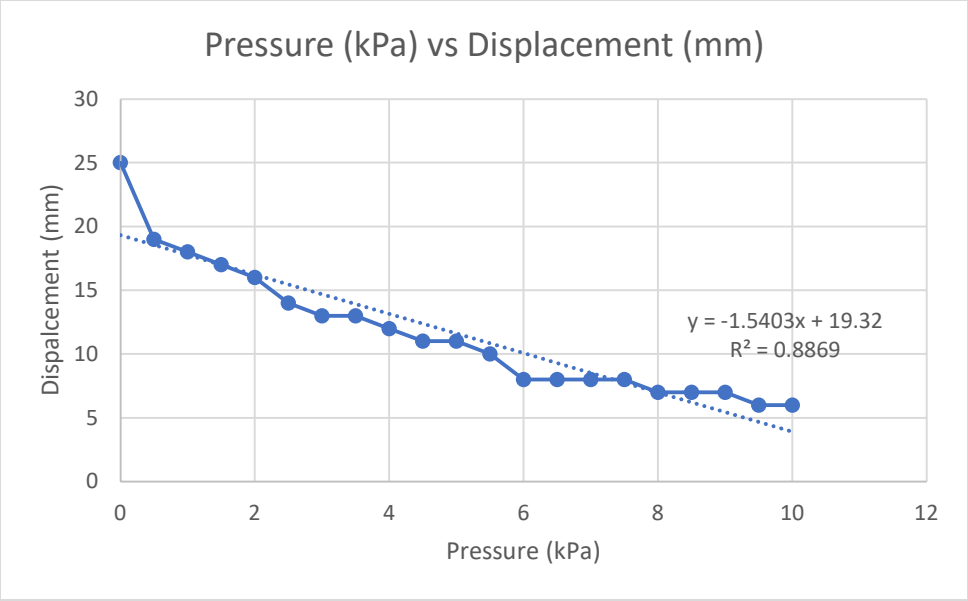

Figure 13: This is the pressure vs displacement of the hanging three-point bending test. The line of best fit, line of best fit equation, and the r-squared value were added through Microsoft Excel.

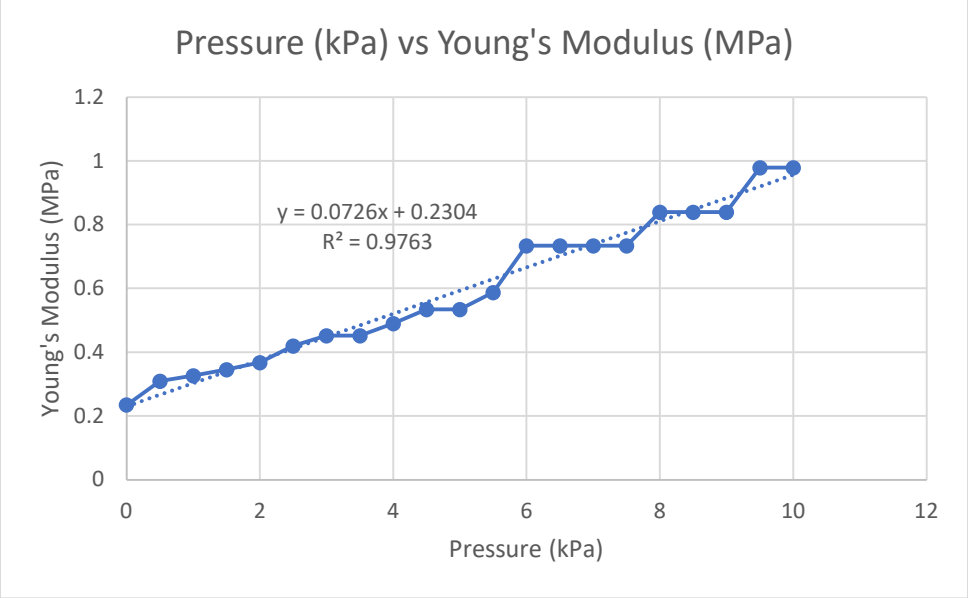

Figure 14: This is the pressure vs Young's Modulus of the impact three-point bending test. The line of best fit, line of best fit equation, and the r-squared value were added through Microsoft Excel.

Discussion

From Figure 13 we see a strong correlation between pressure and displacement as also seen in the impact test. This is expected because it is natural to believe that as the pressure of the jamming increases, the displacement will decrease. On another note, the 0kPa data point apears to be an outlier from the naked eye. This may be because when the balloon has not undergone jamming, the hanging weight causes more displacement by applying constant force, whereas in the impact test there was only one instance of connection. However, by statistical rules, the 0kPa data point lies within 1.5 times the Interquartile Range of the third quartile. So, it is not an outlier. The intercept of the y-axis in Figure 14 comes from the stiffness of balloon tube itself.

From Figure 14 there is no doubt that pressure and Young's Modulus are correlated, in fact, they are almost perfectly linearly correlated. It worth noting that the Young's Modulus of the Hanging Test are significantly greater than in the Impact Test. This is most likely because the Impact Test created more displacement than the Hanging Test did for reasons previously mentioned.

GENERAL DISCUSSION

In the Impact Test, we found that the pressure and stiffness (Young's Modulus) are decently linearly correlated but even more so exponentially correlated. As the pressure increased the stiffness increased more and more by every increment. However, this is most likely due to the velocity of the falling weight and the elastic properties of the materials like the coffee granules and the rubber balloon. The force by Newton's Second Law will remain the same but dropping the weight makes the impact the biggest contributor to the displacement. Similar to how falling from one meter is less damaging than falling from one hundred meters even though the force remains the same.

So, to improve on the Impact Test, the Hanging Test was done. The Hanging Test eliminates the falling velocity and impact as a factor because we simply place the weight onto the balloon. This way the only force that interacts with the jammed balloon is the mass of the weight and gravity. The data from Table 2 shows this to be true because the Young's Modulus throughout each pressure is greater than in the Impact Test or Table 1.

As it relates to how palpation simulators can be consistently jammed to certain stiffnesses, we can now predict how stiff the jamming makes the device by the pressure created by the vacuum used. The values found from the Hanging Test indicate that there is a very strong, almost perfect, linear correlation between the pressure and stiffness of granular jammed systems. This way, future palpation simulators can use the stiffness at the unjammed state and the stiffness at the

maximum jammed pressure to predict how stiff the jamming of the simulator is. Physicians can then tune the palpation simulator to what ever pressure they would like to match the stiffness of the model organ in any given situation. This begs the question: Is it possible to jam the palpation simulators to match the range of stiffnesses organs undergo when healthy and/or diseased?

From the data collected in Table 2, it is reasonable to assume that we can jam a palpation simulator for a range of about 0.2 MPa to 1 MPa (200kPa to 1000kPa). According to the research done by the Memorial Sloan Kettering Cancer Center [91], the liver can vary in stiffness from about 2kPa to 20kPa when healthy to diseased. Kidney tissue ranges from 4kPa when healthy to 100kPa when diseased. Prostate tissue can range from 42kPa when healthy to over 200kPa when diseased [92]. Finally, lungs when healthy are about 6kPa and lung tumors get to be 30kPa [93]. Overall, it seems like the stiffness of the coffee-filled balloons may be too stiff for the simulation of human tissue. Perhaps coffee-granules can simulate prostate palpation tests but most organs would not be valid. It is also worth noting that the size of the organ may be a reason. Since this experiment uses a three-point bending test, the shape and size of the balloon was that of a beam. The balloons used for palpation are more “organ” shaped. The problem with testing with “organ” shaped balloons is it is difficult to test the stiffness of these shapes since they are irregular especially when jammed. A common way to find the stiffness of materials is to apply a tension test where a tensile testing machine pulls the material apart to test its stiffness. But doing this with a coffee-granule filled balloon will most likely be testing the stiffness of the balloon rather than the jammed coffee.

There are a few ways to combat this however. For example, physicians can use the coffee-granule devices to test the difference between stiffnesses of healthy and non-healthy organs. For example, the liver has about a 20kPa difference in stiffness when healthy and diseased. So they can practice finding that specific difference in stiffness. Another idea is to change the granule material. Historically, coffee-grains are the most popular granular jamming material because of its ease of access, irregular granule shape, granule size, and its rigidity. However, it may be poor at mimicing the properties of human tissue.

There were ideas of using other types of granules like water beads to closer mimic human tissue. Water beads are small granule size spheres that have a softer texture than coffee and also have more similar thermal properties to human tissue than coffee. The user may also control the size of the water beads by leaving them in water for more or less time depending on how large or small they need the granules to be. It is expected that they will have a much lower stiffness than coffee grains and perhaps similar to human tissue.

Lastly, the user may be able to use a thicker rubber for their balloon. The balloon used in this experiment was very thin so that the coffee represented most of the stiffness in the test. However, using a thicker rubber can combat the high stiffness range of coffee grains. This was tested once in a study by He et al. [86] where they used a 6.5mm thick balloon to simulate liver tumors. Their stiffness was about 50kPa at the lowest and 125kPa at the maximum which is a lower value as needed but not quite low enough to reach the range of liver stiffness. You can also see

that increasing the thickness of the rubber greately lowers the range of stiffness the jamming can be capable of.

CONCLUSIONS

In this paper, we discuss the correlation between pressure and stiffness in granular jammed devices. We proposed that there is a linear relationship between pressure and stiffness by using three-point bending tests in the lab. We found that over a stiffness range of 200kPa to 1000kPa the pressure increase remains linear almost perfectly. We also found that the stiffness of coffee granules causes the simulation of organs for palpation slightly too large and it may be reasonable to work with other materials for granules. Future work may be focused on how to identify finer jam materials and thinner rubber skin at a similar stiffness as human organs and tissue.

LIST OF REFERENCES

1. Albert I, Sample JG, Morss AJ, Rajagopalan S, Barabási AL, Schiffer P. Granular drag on a discrete object: Shape effects on jamming. Phys Rev E Stat Phys Plasmas Fluids Relat Interdiscip Topics. 2001;64(6).
2. Kahng B, Albert I, Schiffer P, Barabási AL. Modeling relaxation and jamming in granular media. Phys Rev E Stat Phys Plasmas Fluids Relat Interdiscip Topics. 2001;64(5).
3. Giacco F, de Arcangelis L, Pica Ciamarra M, Lippiello E. Rattler-induced aging dynamics in jammed granular systems. Soft Matter. 2017;13(48).
4. Bo L, Mari R, Song C, Makse HA. Cavity method for force transmission in jammed disordered packings of hard particles. Soft Matter. 2014;10(37).
5. Lagubeau G, Rescaglio A, Melo F. Armoring a droplet: Soft jamming of a dense granular interface. Phys Rev E Stat Nonlin Soft Matter Phys. 2014;90(3).
6. Rørvik SB, Auflem M, Dybvik H, Steinert M. Perception by Palpation: Development and Testing of a Haptic Ferrogranular Jamming Surface. Front Robot AI. 2021;8.
7. Chen Y, Yuan M, Wang Z, Zhao Y, Li J, Hu B, et al. Structural characterization and statistical properties of jammed soft ellipsoid packing. Soft Matter. 2021;17(10).
8. Wang K, Song C, Wang P, Makse HA. Edwards thermodynamics of the jamming transition for frictionless packings: Ergodicity test and role of angoricity and compactivity. Phys Rev E Stat Nonlin Soft Matter Phys. 2012;86(1).
9. Potiguar FQ, Makse HA. Effective temperature and jamming transition in dense, gently sheared granular assemblies. European Physical Journal E. 2006;19(2).
10. Farhadi S, Behringer RP. Dynamics of sheared ellipses and circular disks: Effects of particle shape. Phys Rev Lett. 2014;112(14).
11. Krapf NW. Force propagation in isostatic granular packs. Phys Rev E Stat Nonlin Soft Matter Phys. 2012;86(2).
12. Sussman DM, Stenull O, Lubensky TC. Topological boundary modes in jammed matter. Soft Matter. 2016;12(28).
13. Ebrahimnazhad Rahbari SH, Khadem-Maaref M, Seyed Yaghoubi SKA. Universal features of the jamming phase diagram of wet granular materials. Phys Rev E Stat Nonlin Soft Matter Phys. 2013;88(4).
14. Azéma E, Radjaï F, Peyroux R, Richefeu V, Saussine G. Short-time dynamics of a packing of polyhedral grains under horizontal vibrations. European Physical Journal E. 2008;26(3).

15. Berthier L, Chaudhuri P, Coulais C, Dauchot O, Sollich P. Suppressed compressibility at large scale in jammed packings of size-disperse spheres. Phys Rev Lett. 2011;106(12).

16. Donev A, Torquato S, Stillinger FH. Pair correlation function characteristics of nearly jammed disordered and ordered hard-sphere packings. Phys Rev E Stat Nonlin Soft Matter Phys. 2005;71(1).

17. Jorjadze I, Pontani LL, Newhall KA, Brujić J. Attractive emulsion droplets probe the phase diagram of jammed granular matter. Proc Natl Acad Sci U S A. 2011;108(11).

18. Kim K, Moon JK, Park JJ, Kim HK, Pak HK. Jamming transition in a highly dense granular system under vertical vibration. Phys Rev E Stat Nonlin Soft Matter Phys. 2005;72(1).

19. Arévalo R, Zuriguel I, Maza D. Topology of the force network in the jamming transition of an isotropically compressed granular packing. Phys Rev E Stat Nonlin Soft Matter Phys. 2010;81(4).

20. Zhao SC, Schröter M. Measuring the configurational temperature of a binary disc packing. Soft Matter. 2014;10(23).

21. Lefèvre A, Berthier L, Stinchcombe R. Spatially heterogeneous dynamics in a model for granular compaction. Phys Rev E Stat Nonlin Soft Matter Phys. 2005;72(1).

22. Song C, Wang P, Makse HA. Experimental measurement of an effective temperature for jammed granular materials. Proc Natl Acad Sci U S A. 2005;102(7).

23. Paillusson F. Devising a protocol-related statistical mechanics framework for granular materials. Phys Rev E Stat Nonlin Soft Matter Phys. 2015;91(1).

24. Rietz F, Stannarius R. On the brink of jamming: Granular convection in densely filled containers. Phys Rev Lett. 2008;100(7).

25. Yoshioka N, Hayakawa H. Phase transition in peristaltic transport of frictionless granular particles. Phys Rev E Stat Nonlin Soft Matter Phys. 2012;85(3).

26. Newhall J, Cao J, Milner ST. Lattice model of correlated forces in granular solids near jamming. Phys Rev E Stat Nonlin Soft Matter Phys. 2013;87(5).

27. Bi D, Chakraborty B. Rheology of granular materials: Dynamics in a stress landscape. Philosophical Transactions of the Royal Society A: Mathematical, Physical and Engineering Sciences. 2009;367(1909).

28. Sarkar S, Bi D, Zhang J, Ren J, Behringer RP, Chakraborty B. Shear-induced rigidity of frictional particles: Analysis of emergent order in stress space. Phys Rev E. 2016;93(4).

29. Grob M, Heussinger C, Zippelius A. Jamming of frictional particles: A nonequilibrium first-order phase transition. Phys Rev E Stat Nonlin Soft Matter Phys. 2014;89(5).

30. Desmond K, Franklin S v. Jamming of three-dimensional prolate granular materials. Phys Rev E Stat Nonlin Soft Matter Phys. 2006;73(3).

31. Bottinelli A, Sumpter DTJ, Silverberg JL. Emergent Structural Mechanisms for High-Density Collective Motion Inspired by Human Crowds. Phys Rev Lett. 2016;117(22).

32. Jose J, van Blaaderen A, Imhof A. Random three-dimensional jammed packings of elastic shells acting as force sensors. Phys Rev E. 2016;93(6).

33. Iliev PS, Wittel FK, Herrmann HJ. Inversion of force lines in fiber-reinforced jammed granular material. European Physical Journal E. 2021;44(4).

34. Lespiat R, Cohen-Addad S, Höhler R. Jamming and flow of random-close-packed spherical bubbles: An analogy with granular materials. Phys Rev Lett. 2011;106(14).

35. Fierro A, Nicodemi M, Tarzia M, de Candia A, Coniglio A. Jamming transition in granular media: A mean-field approximation and numerical simulations. Phys Rev E Stat Nonlin Soft Matter Phys. 2005;71(6).

36. Otsuki M, Hayakawa H. Critical scaling near jamming transition for frictional granular particles. Phys Rev E Stat Nonlin Soft Matter Phys. 2011;83(5).

37. Haverkamp CB, Hwang D, Lee C, Bartlett MD. Deterministic control of adhesive crack propagation through jamming based switchable adhesives. Soft Matter. 2021;17(7).

38. Smart AG, Ottino JM. Evolving loop structure in gradually tilted two-dimensional granular packings. Phys Rev E Stat Nonlin Soft Matter Phys. 2008;77(4).

39. Silbert LE, Ertaş D, Grest GS, Halsey TC, Levine D. Analogies between granular jamming and the liquid-glass transition. Phys Rev E Stat Phys Plasmas Fluids Relat Interdiscip Topics. 2002;65(5).

40. Majmudar TS, Sperl M, Luding S, Behringer RP. Jamming transition in granular systems. Phys Rev Lett. 2007;98(5).

41. Jose J, Blab GA, van Blaaderen A, Imhof A. Jammed elastic shells-a 3D experimental soft frictionless granular system. Soft Matter. 2015;11(9).

42. Johnsen, Chevalier C, Lindner A, Toussaint R, Clément E, Måløy KJ, et al. Decompaction and fluidization of a saturated and confined granular medium by injection of a viscous liquid or gas. Phys Rev E Stat Nonlin Soft Matter Phys. 2008;78(5).

43. Cheng N, Amend J, Farrell T, Latour D, Martinez C, Johansson J, et al. Prosthetic Jamming Terminal Device: A Case Study of Untethered Soft Robotics. Soft Robot. 2016;3(4).

44. Coulais C, Behringer RP, Dauchot O. How the ideal jamming point illuminates the world of granular media. Soft Matter. 2014;10(10).

45. Ding Y, Gong D, Yang J, Xu Z, Wang Z, Li J, et al. Cubatic structural transformation of the packing of granular cylinders. Soft Matter. 2022;

46. Sikander S, Biswas P, Song SE. Feasibility study and experimental evaluation of the design of nodule prototype developed for palpation display apparatus: A novel device for contactless primary tactile diagnosis. Micromachines (Basel). 2021;12(5).

47. Mowlavi S, Kamrin K. Interplay between hysteresis and nonlocality during onset and arrest of flow in granular materials. Soft Matter. 2021;17(31).

48. Puckett JG, Daniels KE. Equilibrating temperature-like variables in jammed granular subsystems. arXiv:12077349v1. 2012;

49. Corwin EI, Jaeger HM, Nagel SR. Structural signature of jamming in granular media. Nature. 2005;435(7045).

50. Topin V, Radjai F, Delenne JY. Subparticle stress fields in granular solids. Phys Rev E Stat Nonlin Soft Matter Phys. 2009;79(5).

51. Wang P, Song C, Briscoe C, Makse HA. Particle dynamics and effective temperature of jammed granular matter in a slowly sheared three-dimensional Couette cell. Phys Rev E Stat Nonlin Soft Matter Phys. 2008;77(6).

52. Wang Y, Li L, Hofmann D, Andrade JE, Daraio C. Structured fabrics with tunable mechanical properties. Nature. 2021;596(7871).

53. Leblanc KJ, Niemi SR, Bennett AI, Harris KL, Schulze KD, Sawyer WG, et al. Stability of High Speed 3D Printing in Liquid-Like Solids. ACS Biomater Sci Eng. 2016;2(10).

54. Díaz Hernández Rojas R, Parisi G, Ricci-Tersenghi F. Inferring the particle-wise dynamics of amorphous solids from the local structure at the jamming point. Soft Matter. 2021;17(4).

55. Kawasaki T, Coslovich D, Ikeda A, Berthier L. Diverging viscosity and soft granular rheology in non-Brownian suspensions. Phys Rev E Stat Nonlin Soft Matter Phys. 2015;91(1).

56. Park W, Lee D, Bae J. A Hybrid Jamming Structure Combining Granules and a Chain Structure for Robotic Applications. Soft Robot. 2021;

57. Zhang HP, Makse HA. Jamming transition in emulsions and granular materials. Phys Rev E Stat Nonlin Soft Matter Phys. 2005;72(1).

58. Tsai JC, Chou MR, Huang PC, Fei HT, Huang JR. Soft granular particles sheared at a controlled volume: Rate-dependent dynamics and the solid-fluid transition. Soft Matter. 2020;16(32).

59. Richard P, Nicodemi M, Delannay R, Ribière P, Bideau D. Slow relaxation and compaction of granular systems. Vol. 4, Nature Materials. 2005.

60. Wang Y, Wang Y, Zhang J. Connecting shear localization with the long-range correlated polarized stress fields in granular materials. Nat Commun. 2020;11(1).

61. Howard GD, Brett J, O'Connor J, Letchford J, Delaney GW. One-Shot 3D-Printed Multimaterial Soft Robotic Jamming Grippers. Soft Robot. 2021;

62. Mendes BB, Daly AC, Reis RL, Domingues RMA, Gomes ME, Burdick JA. Injectable hyaluronic acid and platelet lysate-derived granular hydrogels for biomedical applications. Acta Biomater. 2021;119.

63. Bandi MM, Rivera MK, Krzakala F, Ecke RE. Fragility and hysteretic creep in frictional granular jamming. Phys Rev E Stat Nonlin Soft Matter Phys. 2013;87(4).

64. Amirifar R, Dong K, Zeng Q, An X. Self-assembly of granular spheres under one-dimensional vibration. Soft Matter. 2018;14(48).

65. Jin Y, Yoshino H. A jamming plane of sphere packings. Proc Natl Acad Sci U S A. 2021;118(14).

66. Berzi D, Buzzaccaro S. A heavy intruder in a locally-shaken granular solid. Soft Matter. 2020;16(16).

67. de Falco I, Gerboni G, Cianchetti M, Menciassi A. Design and fabrication of an elastomeric unit for soft modular robots in minimally invasive surgery. Journal of Visualized Experiments. 2015;2015(105).

68. Amanov E, Nguyen TD, Markmann S, Imkamp F, Burgner-Kahrs J. Toward a Flexible Variable Stiffness Endoport for Single-Site Partial Nephrectomy. Ann Biomed Eng. 2018;46(10).

69. Bi D, Zhang J, Chakraborty B, Behringer RP. Jamming by shear. Nature. 2011;480(7377).

70. Robertson MA, Paik J. New soft robots really suck: Vacuum-powered systems empower diverse capabilities. Sci Robot. 2017;2(9).

71. Jose PP, Andricioaei I. Similarities between protein folding and granular jamming. Nat Commun. 2012;3.

72. Wellborn PS, Russell PT, Webster RJ. A multi-subject accuracy study on granular jamming for non-invasive attachment of fiducial markers to patients. Int J Comput Assist Radiol Surg. 2020;15(1).

73. Cantor D, Cárdenas-Barrantes M, Preechawuttipong I, Renouf M, Azéma E. Compaction Model for Highly Deformable Particle Assemblies. Phys Rev Lett. 2020;124(20).

74. Riley L, Schirmer L, Segura T. Granular hydrogels: emergent properties of jammed hydrogel microparticles and their applications in tissue repair and regeneration. Vol. 60, Current Opinion in Biotechnology. 2019.

75. Simonds E, Colton J, Kogler G, Chang YH. Design and testing of a prototype foot orthosis that uses the principle of granular jamming. Prosthet Orthot Int. 2021;45(3).

76. Vu T lo, Barés J. Soft-grain compression: Beyond the jamming point. Phys Rev E. 2019;100(4).

77. Rhodeland B, Hoeger K, Ursell T. Bacterial surface motility is modulated by colony-scale flow and granular jamming. J R Soc Interface. 2020;17(167).

78. de Falco I, Cianchetti M, Menciassi A. A soft multi-module manipulator with variable stiffness for minimally invasive surgery. Bioinspir Biomim. 2017;12(5).

79. Langer M, Amanov E, Burgner-Kahrs J. Stiffening sheaths for continuum robots. Soft Robot. 2018;5(3).

80. Nampoothiri JN, Wang Y, Ramola K, Zhang J, Bhattacharjee S, Chakraborty B. Emergent Elasticity in Amorphous Solids. Phys Rev Lett. 2020;125(11).

81. Shin M, Song KH, Burrell JC, Cullen DK, Burdick JA. Injectable and Conductive Granular Hydrogels for 3D Printing and Electroactive Tissue Support. Advanced Science. 2019;6(20).

82. Cavallo A, Brancadoro M, Tognarelli S, Menciassi A. A Soft Retraction System for Surgery Based on Ferromagnetic Materials and Granular Jamming. Soft Robot. 2019;6(2).

83. Das P, Vinutha HA, Sastry S. Unified phase diagram of reversible–irreversible, jamming, and yielding transitions in cyclically sheared soft-sphere packings. Proc Natl Acad Sci U S A. 2020;117(19).

84. Porta CAML, Zapperi S. Statistical Features of Collective Cell Migration. In: Advances in Experimental Medicine and Biology. 2019.

85. Choi J, Lee DY, Eo JH, Park YJ, Cho KJ. Tendon-driven jamming mechanism for configurable variable stiffness. Soft Robot. 2021;8(1).

86. He L, Herzig N, de Lusignan S, Nanayakkara T. Granular Jamming Based Controllable Organ Design for Abdominal Palpation. In: Proceedings of the Annual International Conference of the IEEE Engineering in Medicine and Biology Society, EMBS. 2018.

87. Brancadoro M, Manti M, Tognarelli S, Cianchetti M. Fiber Jamming Transition as a Stiffening Mechanism for Soft Robotics. Soft Robot. 2020;7(6).

88. Jiang Y, Chen D, Liu C, Li J. Chain-Like Granular Jamming: A Novel Stiffness-Programmable Mechanism for Soft Robotics. Soft Robot. 2019;6(1).

89. Helps T, Taghavi M, Wang S, Rossiter J. Twisted Rubber Variable-Stiffness Artificial Muscles. Soft Robot. 2020;7(3).

90. He L, Leong F, Lalitharatne TD, de Lusignan S, Nanayakkara T. A Haptic Mouse Design with Stiffening Muscle Layer for Simulating Guarding in Abdominal Palpation Training. In: Proceedings - IEEE International Conference on Robotics and Automation. 2021.

91. "Understanding your liver elastography (Fibroscan®) results," *Memorial Sloan Kettering Cancer Center*. [Online]. Available: https://www.mskcc.org/cancer-care/patient-education/understanding-your-fibroscan-

results#:~:text=Your%20liver%20stiffness%20result%20is,possible%20result%20is%2075%20kPa. [Accessed: 30-Mar-2023].

92. Martinez-Vidal, L., Murdica, V., Venegoni, C. *et al.* **Causal contributors to tissue stiffness and clinical relevance in urology**. *Commun Biol* 4, 1011 (2021). https://doi.org/10.1038/s42003-021-02539-7

93. Ishihara S, Haga H. Matrix Stiffness Contributes to Cancer Progression by Regulating Transcription Factors. Cancers (Basel). 2022 Feb 18;14(4):1049. doi: 10.3390/cancers14041049. PMID: 35205794; PMCID: PMC8870363.